

Supporting Information:

Active and Stable Liquid Water Innovatively Prepared Using Resonantly Illuminated Gold Nanoparticles

Hsiao-Chien Chen,¹ Bing-Joe Hwang,² Fu-Der Mai,^{1,3} Yu-Chuan Liu,^{1,3*} Chun-Mao Lin,¹ Hsien-Shou Kuo,¹ Duen-Suey Chou,⁴ Ming-Jer Lee,² Kuang-Hsuan Yang,⁵ Chung-Chin Yu,⁶ Jiun-Rong Chen,⁷ Tsui-Yun Lo,¹ Hui-Yen Tsai,¹ Chih-Ping Yang,⁸ Chi Wang,⁸ Hsiao-Ting Hsieh,⁸ John Rick²

¹Department of Biochemistry, School of Medicine, College of Medicine, Taipei Medical University, No. 250, Wu-Hsing St., Taipei 11031, Taiwan

²Department of Chemical Engineering, National Taiwan University of Science and Technology, No. 43, Sec. 4, Keelung Rd., Taipei 10607, Taiwan

³Biomedical Mass Imaging Research Center, Taipei Medical University, No. 250, Wu-Hsing St., Taipei 11031, Taiwan

⁴Department of Pharmacology, School of Medicine, College of Medicine, Taipei Medical University, No. 250, Wu-Hsing St., Taipei 11031, Taiwan

⁵Department of Materials Science and Engineering, Vanung University, No. 1, Van Nung Rd., Chung-Li City, Taiwan

⁶Department of Environmental Engineering, Vanung University, No. 1, Van Nung Rd., Chung-Li City, Taiwan

⁷School of Nutrition and Health Sciences, Taipei Medical University, No. 250, Wu-Hsing St., Taipei 11031, Taiwan

⁸Graduate Institute of Medical Science, College of Medicine, Taipei Medical University, No. 250, Wu-Hsing St., Taipei 11031, Taiwan

* Address correspondence to: liuyc@tmu.edu.tw

MATERIALS AND METHODS

UV-vis Spectra of Au NPs and Au NPs-Adsorbed Ceramic Particles.

Ultraviolet-visible absorption measurement for Au NPs in solution was carried out on a Perkin-Elmer Lambda 800/900 spectrophotometer in 1-cm quartz cuvette. In experiment, water was used as the background reference and the scan rate was 750 nm min⁻¹. For measuring the spectrum of the solid Au NPs-adsorbed ceramic particles based on a reflection model the spectrophotometer was equipped with a collector of integrating sphere. Wetted ceramic particles were used as the background reference in experiment.

Preparation Conditions of AuNT Water. In preparations deionized (DI) water (pH 7.23, T = 23.5 °C) flew through the glass tube filled with Au NPs-adsorbed ceramic particles under illumination. The time for water flowing through the glass tube is ca. 1500 s for both fluorescent lamp with full visible wavelength and green light-emitting diodes (LED, wavelength maxima centered at 530 nm). Then the AuNT water (pH 7.25, T = 23.3 °C) was collected in glass sample bottles for subsequent measurements in 2 h. For examining the purity of the prepared AuNT water further inductively coupled plasma-mass spectrometer (ICP-MS) analyses indicated that the concentrations of the slightly dissolved metals in the AuNT water are ca. 0.62, 43, 25, 23, 13, 4.5 and 0.41 ppb for Au, Na, K, Al, Mg, Ca and Fe, respectively. Excluding Au, the total equivalent molar concentration of these dissolved metals is equal to 6.9×10^{-6} M. This measured value is ca. 2.4×10^{-7} M for DI water as a reference.

Raman Spectra Recorded on Water and Their Deconvolutions. In measurement prepared water was sealed in a 0.5 mL cell with glass window. Raman spectra were recorded (Micro Raman spectrometer, Model RAMaker) by using a confocal microscope employing a DPSS laser operating at 532 nm with an output power of 1 mW on the sample. A 50x, 0.36 NA Olympus objective (with a working distance of 10 mm) was used to focus the laser light on the samples. The laser spot size is ca. 2.5 μm. A thermoelectrically cooled Andor iDus charge-coupled device (CCD) 1024 x 128 pixels operating at -40 °C was used as the detector with 1 cm⁻¹ resolution. All spectra were calibrated with respect to silicon wafer at 520 cm⁻¹. In measurements, a 180° geometry was used to collect the scattered radiation. A 532 notch filter was used to filter the excitation line from the collected light. The acquisition time for each measurement was 1 s. Thirty sequential measurements were collected for each sample. These Raman spectra were further deconvoluted into five

Gaussian sub-bands based on the methods shown in the literature.¹⁻³ In deconvolution the five-Gaussian components with the center wavenumbers at 3018, 3223, 3393, 3506 and 3624 cm^{-1} were adopted for all samples. Moreover, the full width at half maximum (FWHM) of the individual component in the five-Gaussian fit was equal for all samples. These values are 234, 201, 176, 145 and 112 cm^{-1} for bands at 3018, 3223, 3393, 3506 and 3624 cm^{-1} , respectively. The qualities of these fitted spectra are satisfactory.

FTIR Spectra Recorded on Water. In measurement prepared water was injected into a precision demountable cell (International Crystal Laboratories) for liquid sample. A teflon spacer with a thickness of 0.015 mm was employed. The Fourier transform infrared (FTIR) spectra were measured on a model Bruker-Tensor 27 spectrophotometer with a resolution of 4 cm^{-1} . Thirty-two sequential measurements were collected for each sample.

Saturated Solubility of Solute and Maximum Content of Dissolved Oxygen in Water. The solubility of NaCl in water was obtained by dissolving excess NaCl in 20 mL water under stirring for 30 min. Then the solution is stirless for another 30 min. Subsequently, five samples of 1 mL of the clear NaCl-saturated solution were weighted. The saturated solubility of NaCl based on 1 dL water can be calculated by utilizing the known densities of 2.165 and 1 for g cm^{-3} for NaCl and water, respectively. The relative deviation of individual value from the average value is less than 3 %. In measurement for Tapimycin, 1.2 g sample was placed in a sample cell. Then water was slowly dropped into the sample cell under stirring until no dissolved sample powder was observed and the solution became transparent colloidal solution. The saturated solubility of Tapimycin based on 1 dL water can be calculated by utilizing the measured mass of 1.2 g and used volume of water (1 g cm^{-3}). Replicate measurements of three times were performed. The relative deviation of individual value from the average value is less than 10 %. In measurement of maximum content of dissolved oxygen in water, pure oxygen was bubbled into 40 mL water in a 50 mL sample cell without sealing for 30 min and then stopped bubbling under sealing for another 5 min. Immediately, the maximum dissolved oxygen in water was recorded on a oxygen-dissolved meter (DO-5510, Lutron electronic enterprise Co., Ltd., Taiwan). Replicate measurements of three times were performed. The relative deviation of individual value from the average value is less than 5 %.

Saturated Vapor Pressure of Water at 25 °C. A static vapor-liquid-liquid equilibrium (VLLE) apparatus was used to measure the VLLE data. The equipment is

similar to that reported in the literature.⁴ The heart of the apparatus is a visual equilibrium cell that is immersed in a visibility thermostatic bath (Model- TV 4000, stability = ± 0.03 K, Neslab, USA). The phase behavior in the equilibrium cell can be observed through the transparent windows. Bath temperature is measured by a precision thermometer (Model-1560, Hart Scientific, USA) with a platinum RTD probe to an accuracy of ± 0.02 K. A pressure transducer (Model, PDCR-912, 0-1000 kPa, Druck, UK) with a digital indicator (Model DPI-261, Druck, UK) measures the equilibrium pressure. The accuracy of the pressure measurement is about ± 0.1 %. A proper amount of solution is loaded in the degassing unit at the beginning of an experiment. The degassing procedure is similar to that reported in the literature.⁵ The degassed solution is then transferred into the equilibrium cell, in which the levels of the vapor-liquid-liquid interfaces should be adjusted properly such that the upper liquid phase can be circulated. Both liquid and vapor mixtures are circulated alternatively by the circulation pumps to promote equilibration. While the system reaches equilibrium, the pressure reading of the cell approaches a constant.

Evaporation Rate of Water in Ambient Laboratory Air. Two samples of 80 mL DI water were individually added in glass beakers (250 mL), which were placed on a platform of an orbital shaker under illumination of fluorescent lamp together, operating at 150 rpm. In one beaker, it contained Au NPs-adsorbed ceramic particles (ca. 20 mL) at the bottom for preparation of AuNT water. In the other beaker, it represents a blank experiment for DI water. The weight of each beaker, containing water or water and Au NPs-adsorbed ceramic particles, was measured every hour for 7 h to determine the evaporating mass (g) of water per hour.

Swelling Test of Artificial Skin on Water. Two pieces of dry and pre-weighted artificial skins (product no. 412021, ConvaTec Inc., USA) of 0.5×0.5 cm² were individually immersed in DI water and AuNT water for 1 h. Then the excess water on the surfaces of skins was quickly and slightly wiped off by using experimental wiper paper (Kimwipes[®]). Subsequently, the wet skins were weighted. The degree of swelling of artificial skin is defined as follows, which was generally shown in the literature.⁶

$$\text{Degree of swelling} = (\text{wet weight} - \text{dry weight}) / (\text{dry weight}) \times 100 \% \quad (2)$$

Chemical Activity of Water in Reduction Preparation of Au NPs. First, ca. 500 ppm Au-containing complex was electrochemically prepared in DI water by using the

similar method shown in a previous report.⁷ Typically in preparation of Au-containing complex, the Au electrode was cycled in a deoxygenated aqueous solution containing 1 N NaCl from -0.28 V (holding 10 s) to 1.22 V (holding 5 s) at 500 mV s⁻¹ for 500 scans. Then 8 mL DI water or AuNT water was mixed with 2 mL of the prepared Au complex-containing solution in a glass sample cell (20 mL). The final concentration of the Au-containing complex in solution was 100 ppm. Subsequently, 10 mg Ch was added in the mixed solution for capping the Au-containing complex under slight stirring for 10 min. Finally, the samples were sealed and placed in ambient laboratory air for further reaction. Generally, the used Ch can be dissolved in an acidic solution. In this experiment, the pH of the solution is ca. 6.7. Thus, the Ch-capped Au complex was settled down without stirring.

Measurement of Free Radicals by Electron Spin Resonance Spectroscopy. In electron spin resonance (ESR) measurement, a Bruker EMX ESR spectrometer was employed. ESR spectra were recorded at room temperature using a quartz flat cell designed for solutions. The dead times between sample preparation and ESR analysis were exactly 1.5 and 10 min for experiments in hydroxyl and DPPH free radicals, respectively, after the last addition. Conditions of ESR spectrometry were as follows: 20 mW power at 9.78 GHz, with a scan range of 100 G and a receiver gain of 6.32×10^4 .

Sample Preparation for Measuring Hydroxyl Free Radicals. The hydroxyl free radicals were obtained by using the well-known Fenton reaction, in which ferrous iron donates an electron to hydrogen peroxide to produce the hydroxyl free radical.^{8,9} Because the produced hydroxyl free radicals are very unstable they are capped by spin-trapping using DMPO to form more stable complex radicals for exact detection. The sample preparation is described as follows. First, 140 μ L DI water or AuNT water was added in a microtube (Eppendorf). Then 20 μ L PBS (10X) was added in the tube. A complex of EDTA-chelated iron(II) was prepared by mixing 0.5 mM iron(II) chloride tetrahydrate and 0.5 mM EDTA with equal volume. Subsequently, 20 μ L EDTA-chelated iron(II) (0.25 mM), 10 μ L H₂O₂ (0.2 mM) and 10 μ L DMPO (2 M) were sequentially added in the tube. The final volume in the tube is 200 μ L. Exact 1.5 min later from the addition of DMPO ESR analysis was performed. To obtain an ESR spectrum, sample was scanned for ca. 1.5 min, accumulated 8 times, and all signals were averaged.

Sample Preparation for Measuring DPPH Free Radicals. Compared to hydroxyl free radicals DPPH is a kind of stable free radicals. The sample preparation

is described as follows. DPPH was dissolved in methanol to prepare 4 mM DPPH solution. Water with different volume ratio of AuNT water in DI water was also prepared. Then the prepared DPPH solution and water were mixed (100 μ L each) in a microtube. The final concentration of DPPH in solution is 2 mM. Exact 10 min later from the mixing of DPPH and water ESR analysis was performed. In measuring an ESR spectrum, sample was scanned for 1 time (ca. 42 s).

LPS-Induced Nitric Oxide Release in Culture Medium. Determination of nitric oxide (NO) production was made following the method shown in the literature.¹⁰ DI water and AuNT water were respectively used for medium preparation. RAW 264.7 cells, a murine macrophage cell line, were obtained from American Type Culture Collection (ATCC) and cultured at 37 °C in Dulbecco's Modified Essential Medium supplemented with 10% fetal bovine serum (FBS), 100 units mL^{-1} penicillin, 100 $\mu\text{g mL}^{-1}$ streptomycin, and 5% CO_2 in incubation chamber as recommended by ATCC. Briefly, RAW 264.7 cells grown on a 10 cm culture dish were seeded in 96-well plates at a density of 2×10^5 cells/well. Adhered cells were then stimulated with various concentrations (0-100 ng mL^{-1}) of E. coli LPS for 24 h. Nitrite in culture medium was measured by adding 100 μL of Griess reagent (1% sulfanilamide and 0.1% N-[1-naphthyl]-ethylenediamine dihydrochloride in 5% phosphoric acid) to 100 μL samples of the medium for 10 min at room temperature. The optical density at 570 nm was measured using a Multiskan RC photometric microplate reader (Labsystems, Helsinki, Finland). A NO standard curve was made with sodium nitrite. The levels of NO production were normalized to cell viability.

ADDITIONAL DISCUSSIONS

DNHBWs on Differently Treated Water. As demonstrated in Table 1 of main text, the DNHBW of AuNT water without illumination of light is 21.50 %, which is very close to the value of DI water. This water was obtained by using the similar preparation condition used in the preparation of the AuNT water, but the experiment was performed in dark. It indicates that illumination of light is necessary for the preparation of SWC water. The DNHBW of AuNT water prepared under illumination of green LED light is 26.23 %, which is far higher than the value of AuNT water. It reveals that resonant light from green LED is more capable for effective preparation of SWC water. Ag or Pt NPs instead of Au NPs were also employed in the preparation of SWC water under illuminations of fluorescent lamps. The results are also positive. The values of DNHBW are 24.36 and 24.23 % based on Ag and Pt NPs, respectively. As shown in the literature,^{11,12} photocatalytic splitting of water was observed on the surfaces of Au-decorated TiO₂ NPs. In this work, Au/TiO₂ nanocomposites instead of Au NPs were also employed in the preparation of SWC water under illumination of fluorescent lamps. The corresponding DNHBW is 24.17 %, which is very close to the value of AuNT water. It indicates that the photocatalyst of TiO₂ helps less for the preparation of SWC water in our system. It is well known, the catalytic activity of supported Au NPs is higher than that of unsupported Au NPs. In this work, Au NPs are adsorbed on ceramic particles, in which the main component is SiO₂. Therefore, Au NPs were deposited on an Au substrate (4 × 4 cm) by using electrochemical oxidation-reduction cycles (ORC; 500 cycles were used in this experiment)¹³ to examine the supporting effect on the corresponding DNHBW. This Au NPs-deposited substrate was immersed in 20 mL DI water in a glass bottle. Then the bottle was placed on a shaking platform under illumination of fluorescent lamps for 2 h. The corresponding DNHBW is 22.86 %, which is higher than the value of DI water. It reveals that Au NPs themselves can break down hydrogen bonds of water under illumination of resonant light to form SWC. Moreover, to examine the influence of the mixing process between DI and AuNT water on the DNHBW, Raman spectra were recorded on the mixing water by adding different volumes of AuNT water in DI water. Basically, it demonstrates a linear relationship between DNHBW and the corresponding ratio, as shown in Figure S1. It reveals that the mixing process belongs to a physical process and DNHBW defined in this work is a reliable index on the evaluation of SWC.

We also carried out the kinds of experiments on D₂O that are routinely done to assess the degree of hydrogen bonding in H₂O water. The experimental results indicate that the values of DNHBW based on D₂O are 23.24, 24.15 and 25.00 % for

untreated D₂O, AuNT D₂O and super SWC derived D₂O, respectively, as shown in Table S1 and Figure S2. The definition of DNHBW is the same as used in water based on H₂O, however, the five Gaussian sub-bands are based on O-H stretching (2700~3900 cm⁻¹) and O-D stretching (2000~3000 cm⁻¹) for H₂O and D₂O, respectively. The definitions of AuNT and super SWC are the same as used in water based on H₂O. In deconvolution the five-Gaussian components with the center wavenumbers at 2267, 2372, 2488, 2589 and 2677 cm⁻¹ were adopted for all D₂O samples. Moreover, FWHM of the individual component in the five-Gaussian fit was equal for all D₂O samples. These values are 149, 118, 134, 143 and 123 cm⁻¹ for bands at 2267, 2372, 2488, 2589 and 2677 cm⁻¹, respectively. The qualities of these fitted spectra are satisfactory. The sub-bands on the low and high frequency sides are related to strong and weak hydrogen-bonded OD features, respectively, as shown in the literature.^{14,15} Although the hydrogen bond in D₂O is stronger than that in H₂O the DNHBW can be also increased from 23.24 to 24.15 % by utilizing the LSPR effect from the ceramic supported Au NPs. This is an increase of ca. 3.9 % for the DNHBW. This increase can be enhanced to 7.6 % by using super SWC.

Saturated Solubility of Solutes and Content of Maximum Dissolved Oxygen in Water. As demonstrated in Table S2, the saturated solubility of NaCl in DI water at room temperature is 36.2 g d L⁻¹, which is very close to the well-known value of 36.0 g d L⁻¹ at 25 °C. Interestingly, this saturated solubility is 41.3 g d L⁻¹ in AuNT water. It is an increase of 14 % of magnitude, as compared with the value measured in DI water. Moreover, based on the AuNT water prepared under LED illumination, this increase can be further improved to 22 % of magnitude. Also, the saturated solubility of Tapimycin (a kind of antibiotic) can be significantly increased by 35 % of magnitude when DI water was replaced by AuNT water in experiment. Moreover, based on the AuNT water prepared under LED illumination, this increase can be further improved to 51 % of magnitude. These results indicate that both electrolyte and colloid can be more effectively dissolved in AuNT water with SWC. Moreover, the dissolution of oxygen was also investigated to evaluate the enhanced capacity in carrying oxygen for AuNT water. As demonstrated in Table S2, the maximum content of dissolved O₂ in DI water at room temperature is 20.3 mg L⁻¹. Interestingly, this value was measured to be 23.8 mg L⁻¹ in AuNT water. It is an increase of 17 % of magnitude, as compared with the value measured in DI water. More free water in the AuNT water with weaker hydrogen bonding, which can more effectively interact with dissolved O₂ by hydrogen-bonding, is responsible for this result. Based on the AuNT water prepared under LED illumination, this increase can be improved to 36 % of magnitude, as expected, due to more free water available.

Vapor pressures of AuNT and DI water. As shown in Table S3, at beginning, the vapor pressures were 0.0208 and 0.0327 bar for DI water and AuNT water, respectively. It revealed that the AuNT water with SWC evaporated instantaneously. After 6 h, the saturated vapor pressures were 0.0316 and 0.0344 bar for DI water and AuNT water, respectively. It indicated that the saturated vapor pressure of AuNT water is significantly higher than that of DI water.

Evaporation Rates and Heating Time for Boiling of AuNT and DI Water. As shown in Figure S3, in the first hour, the evaporation rate of AuNT water is increased by ca. 3.5 % of magnitude, as compared with that of DI water. Finally, in the 6th to 7th hours, this increase has been enhanced to ca. 12 to 13 %, which is very close to the corresponding increase of DNHBW of 13 %. Based on this distinct property of AuNT water, time for heating water (50 mL water in 100 mL beaker) from room temperature to its boiling point was also investigated. Experimental results reveal that ca. 6, 5 and 4.5 min are necessary for boiling DI water, AuNT water and AuNT water prepared under illumination of LED, respectively, in the same heating condition. As expected, AuNT water with weaker hydrogen bonding boils faster than DI water does.

Contact Angles and Penetration Abilities of AuNT and DI Water. The contact angles of DI water and AuNT water on artificial skins are shown in Figure S4. At beginning, the contact angles are 89.7° and 83.5° for DI water and AuNT water, respectively. It reveals that the cohesion of AuNT water with weaker hydrogen bonding is weaker than that of DI water. Also, the contact angles on general glass slides are 47.9°, 48.3° and 41.7° for DI, CPT and AuNT water, respectively. The results are consistent with those observed on the artificial skins and discussed in the Raman spectra. After 10 min, the contact angles on artificial skins are slightly and greatly deduced to 80.8° and 44.9° for DI water and AuNT water, respectively. Moreover, the volume of AuNT water is significantly reduced on the artificial skin after 10 min. Because the diameter of the drop is unchanged this reduction in drop volume could not be ascribed to the evaporation of water. Easy penetration into artificial skin for AuNT water should be responsible for this phenomenon.

Chemical Activity of AuNT Water in Reduction. As shown in Figure S5, the absorbance maximum band of the electrochemically prepared Au-containing complex without Ch appears at ca. 312 nm. This absorbance band disappears when the solution was diluted with both DI water and AuNT water and Ch was added in the diluted solution because most of the yellow Ch-capped Au complex was settled down in the

neutral solution. Encouragingly, after 3 days, the color of the settlement in the AuNT water-containing solution became wine-red. Also, the absorbance maximum band of the solution appears at ca. 522 nm, as shown in spectrum (E) of Figure S5. It indicates that the Au NPs have been successfully prepared¹⁶ under the assistance of reducing agent of AuNT water. As reported by Vohringer-Martinez *et al.*,¹⁷ radical-molecule gas-phase reaction could be catalyzed by water molecules through their ability to form hydrogen bonds. Small gas-phase water clusters could bind an excess electron through a double hydrogen-bond acceptor motif.¹⁸ However, this distinct chemical activity of liquid water is less discussed in the literature. It opens a new green pathway in chemical reduction. We think more free water available in the AuNT water with weaker hydrogen bonding should be responsible for this distinct activity. After 5 days, the color of the settlement in the DI water began changing into pink one. However, there is still no absorbance maximum band in the solution that can confirm the existence of Au NPs, as shown in spectrum (F) of Figure S5. At that time, the absorbance maximum band of the AuNT water-containing solution shifts from 522 to 524 nm, as shown in spectrum (G) of Figure S5. This red shift in spectrum results from the aggregation of Au NPs because more Au NPs have been produced in the solution after 5 days.

REFERENCES

1. Li, R.; Jiang, Z.; Guan, Y.; Yang, H.; Liu, B. Effects of Metal Ion on the Water Structure Studied by the Raman O[BOND]H Stretching Spectrum. *J. Raman Spectrosc.* **2009**, *40*, 1200-1204.
2. Carey, D. M.; Korenowski, G. M. Measurement of the Raman Spectrum of Liquid Water. *J. Chem. Phys.* **1998**, *108*, 2669-2775.
3. Sun, Q. Raman Spectroscopic Study of the Effects of Dissolved NaCl on Water Structure. *Vib. Spectrosc.* **2012**, *62*, 110-114.
4. Lee, M. J.; Tsai, L. H.; Hong, G. B.; Lin, H. M. Multiphase Coexistence for Aqueous Systems with Amyl Alcohol and Amyl Acetate. *Ind. Eng. Chem. Res.* **2002**, *41*, 3247-3252.
5. Lee, M. J.; Hu, C. H. Isothermal Vapor-Liquid Equilibria for Mixtures of Ethanol, Acetone, and Diisopropyl Ether. *Fluid Phase Equilib.* **1995**, *109*, 83-98.
6. Karaborni, S.; Smit, B.; Heidug, W.; Urai, J.; van Oort, E. The Swelling of Clays: Molecular Simulations of the Hydration of Montmorillonite. *Science* **1996**, *271*, 1102-1104.
7. Liu, Y. C.; Yu, C. C.; Yang, K. H. Active Catalysts of Electrochemically Prepared Gold Nanoparticles for the Decomposition of Aldehyde in Alcohol Solutions. *Electrochem. Commun.* **2006**, *8*, 1163-1167.
8. Ohsawa, I.; Ishikawa, M.; Takahashi, K.; Watanabe, M.; Nishimaki, K.; Yamagata, K.; Katsura, K.; Katayama, Y.; Asoh, S.; Ohta, S. Hydrogen Acts as A Therapeutic Antioxidant by Selectively Reducing Cytotoxic Oxygen Radicals. *Nat. Med.* **2007**, *13*, 688-694.
9. Liu, Y.; Imlay, J. A. Cell Death from Antibiotics without the Involvement of Reactive Oxygen Species. *Science* **2013**, *339*, 1210-1213.
10. Lin, H. C.; Tsai, S. H.; Chen, C. S.; Chang, Y. C.; Lee, C. M.; Lai, Z. Y.; Lin, C. M. Structure–Activity Relationship of Coumarin Derivatives on Xanthine Oxidase-Inhibiting and Free Radical-Scavenging Activities. *Biochem. Pharmacol.* **2008**, *75*, 1416-1425.
11. Lee, M. J.; Ji, S.; Stucky, X. G. D.; Moskovits, M. Plasmonic Photoanodes for Solar Water Splitting with Visible Light. *Nano Lett.* **2012**, *12*, 5014-5019.
12. Silva, C. G.; Juarez, R.; Marino, T.; Molinari, R.; Garcia, H. Influence of Excitation Wavelength (UV or visible light) on the Photocatalytic Activity of Titania Containing Gold Nanoparticles for the Generation of Hydrogen or Oxygen from Water. *J. Am. Chem. Soc.* **2011**, *133*, 595-602.

13. Liu, Y. C. Evidence of Chemical Effect on Surface-Enhanced Raman Scattering of Polypyrrole Films Electrodeposited on Roughened Gold Substrates. *Langmuir* **2002**, *18*, 174-181.
14. Ahmed, M.; Singh, A. K.; Mondal, J. A.; Sarkar, S. K. Water in the Hydration Shell of Halide Ions Has Significantly Reduced Fermi Resonance and Moderately Enhanced Raman Cross Section in the OH Stretch Regions. *J. Phys. Chem. B* **2013**, *117*, 9728-9733.
15. Sastry, M. I. S. Singh, S. Derivative Analysis of Raman Spectra of Liquid Water in the O-H (D) Stretching Region. *J. Mol. Struct.* **1987**, *158* 195-204.
16. Dawson, A.; Kamat, P. V. Semiconductor–Metal Nanocomposites. Photoinduced Fusion and Photocatalysis of Gold-Capped TiO₂ (TiO₂/Gold) Nanoparticles. *J. Phys. Chem. B* **2001**, *105*, 960-966.
17. Vöhringer-Martinez, E.; Hansmann, B.; Hernandez, H.; Francisco, J. S.; Troe, J.; Abel, B. Water Catalysis of A Radical-Molecule Gas-Phase Reaction. *Science* **2007**, *315*, 497-501.
18. Hammer, N. I.; Shin, J. W.; Headrick, J. M.; Diken, E. G.; Roscioli, J. R.; Weddle, G. H.; Johnson, M. A. How Do Small Water Clusters Bind an Excess Electron? *Science* **2004**, *306*, 675-679.

Table S1. Ratios of five-Gaussian components of OD stretching Raman bands and degree of nonhydrogen-bonded water (DNHBW) for various pure water of D₂O.

Sample	(1) 2267 cm ⁻¹ (%)	(2) 2372 cm ⁻¹ (%)	(3) 2488 cm ⁻¹ (%)	(4) 2589 cm ⁻¹ (%)	(5) 2677 cm ⁻¹ (%)	DNHBW (%)
a	4.76	34.30	37.70	17.95	5.29	23.24
b	4.62	34.05	37.18	18.83	5.32	24.15
c	3.00	33.64	38.36	19.16	5.84	25.00

Various samples of pure water of D₂O: (a) D₂O; (b) AuNT D₂O; (c) super SWC water of D₂O.

Table S2. Saturated solubilities of solutes and content of maximum dissolved oxygen in various pure water (1 atm and water temperature of 22.8 °C).

	NaCl (g d L ⁻¹)	Tapimycin (antibiotic) (g d L ⁻¹)	O ₂ (mg L ⁻¹)
DI water	36.2	104.5	20.3
^a AuNT water	41.3	140.6	23.8
^b AuNT water	44.0	158.2	27.7

^aAuNT water prepared under illumination of fluorescent lamp.

^bAuNT water prepared under illumination of green LED light.

Table S3. Saturated vapor pressures of DI water and AuNT water at 25 °C.

	0 min (bar)	30 min (bar)	3 h (bar)	6 h (bar)
DI water (24.8 °C)	0.0208	0.0313	0.0313	0.0316
AuNT water (24.7 °C)	0.0327	0.0356	0.0354	0.0344

Note: Saturated vapor pressure of water is 0.0317 bar at 25 °C according to steam table.

Table S4. Degree of swelling of artificial skin by using DI or AuNT water.

	Dry weight (g)	Wet weight (g)	Degree of swelling (%)
DI water	0.1217	0.1332	9.45
AuNT water	0.1328	0.1485	11.8

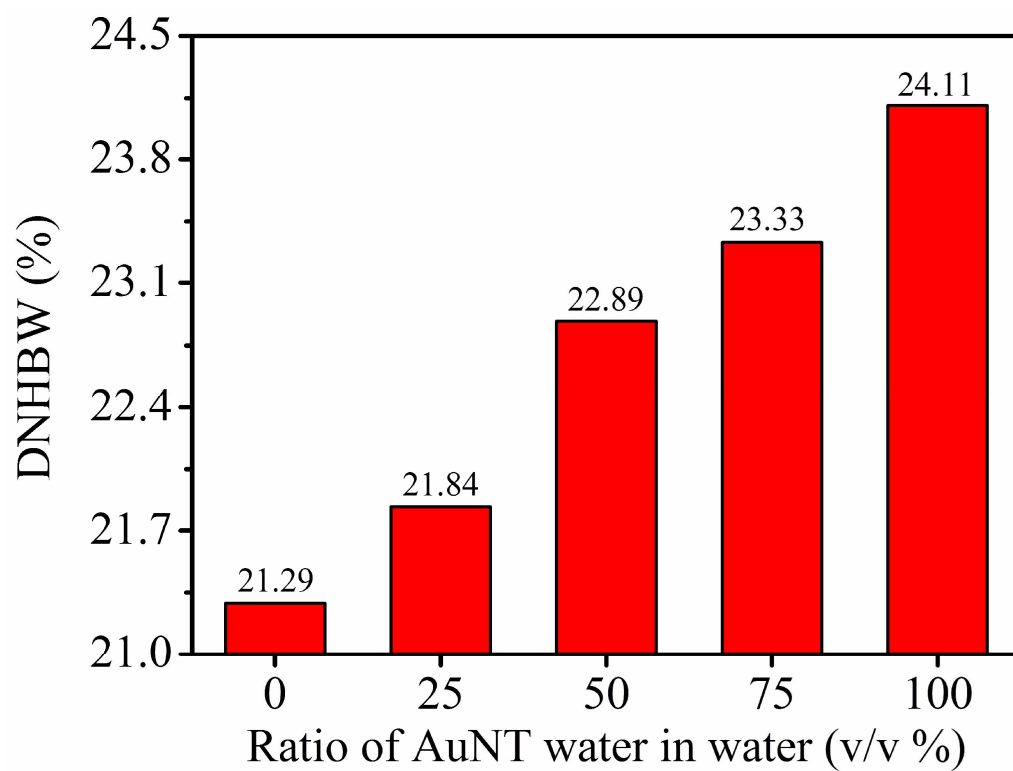


Figure S1. DNHBW of water composed of different ratios of AuNT water in water.

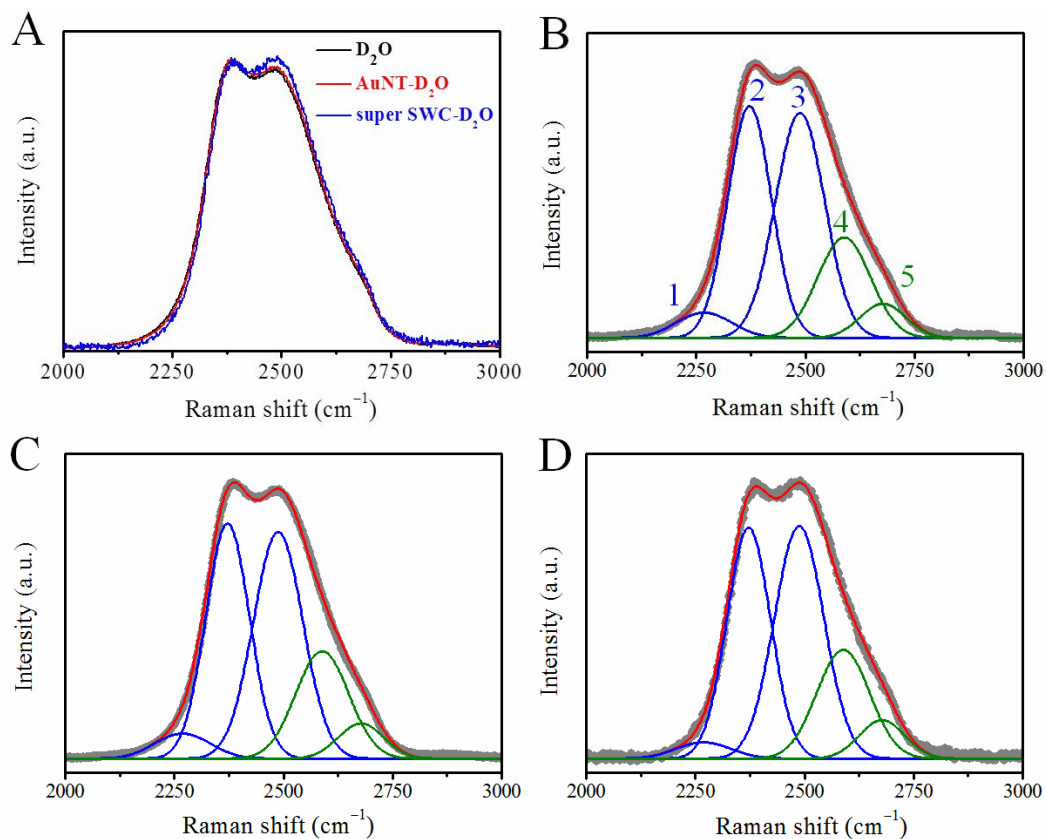


Figure S2. Raman spectra of OD stretching of various water of D₂O: (A) Original Raman spectra for untreated D₂O, AuNT D₂O and super SWC derived D₂O. (B) Five Gaussian sub-bands of D₂O for reference. (C) Five Gaussian sub-bands of AuNT D₂O, which was prepared under illumination of green LED light. (D) Five Gaussian sub-bands of super small water-clusters (SWC) derived D₂O; this super SWC Raman spectrum was obtained by irradiating D₂O-wetted ceramic-supported Au NPs with laser light at 532 nm under *in situ* Raman experiment.

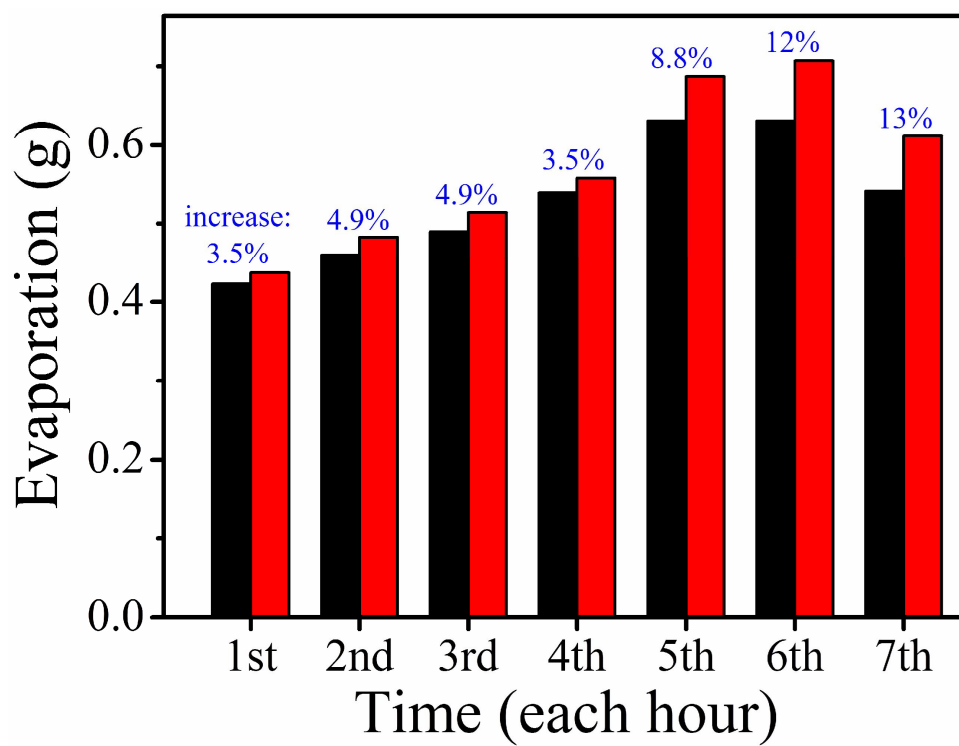


Figure S3. Evaporation rates (g h^{-1}) of DI water (black block) and AuNT water (red block) at 1 atm and room temperature.

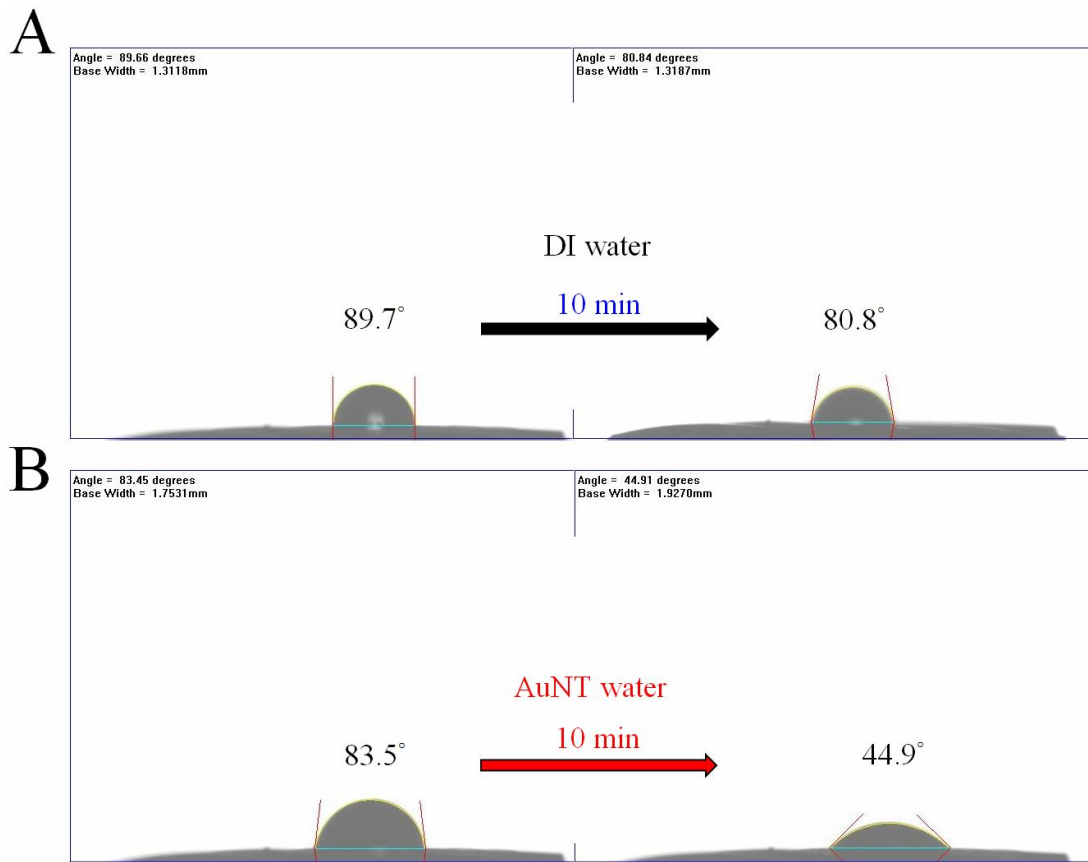


Figure S4. Contact angles of DI water (A) and AuNT water (B) on artificial skins with time.

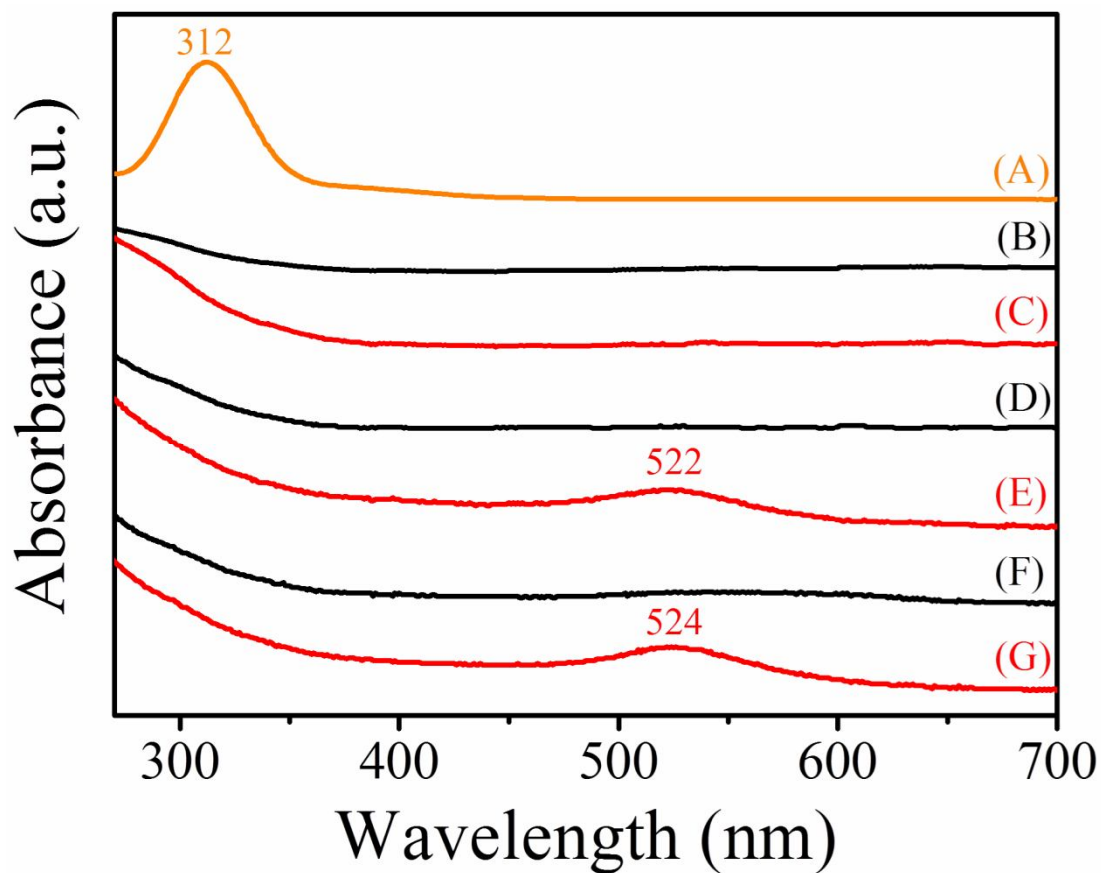


Figure S5. UV-vis absorption spectra of precursors of Au NPs (orange line, spectrum A), obtained Au NPs in DI water with chitosan (black lines, spectra B, D and F for experiments after 0, 3 and 5 days, respectively) and in AuNT water with chitosan (red line, spectra C, E and G for experiments after 0, 3 and 5 days, respectively) with time.